11th World Congress on Computational Mechanics (WCCM XI)
5th European Conference on Computational Mechanics (ECCM V)
6th European Conference on Computational Fluid Dynamics (ECFD VI)
E. Oñate, J. Oliver and A. Huerta (Eds)

THE USE OF FINITE ELEMENT ANALYSIS ON BENDING RADIUS AND SPRINGBACK PREDITION ON CNC PRESS BRAKES PROGRAMING

SARA MIRANDA[1], J. BESSA PACHECO[1], ABEL D. SANTOS[1,2] RUI AMARAL[2]

[1] Faculty of Engineering, University of Porto (FEUP)
Rua Dr. Roberto Frias 400, 4200-465 Porto, Portugal
e-mail: em09194@fe.up.pt, jpacheco@fe.up.pt, abel@fe.up.pt

[2] Institute of Mech. Eng. And Ind. Management (INEGI), University of Porto
Rua Dr. Roberto Frias 400, 4200-465 Porto, Portugal
email: abel@inegi.up.pt, ramaral@inegi.up.pt

Key Words: *Metal Forming, Sheet Metal Bending, Air Bending.*

Abstract. *Sheet metal bending is a metal forming process with a simple geometric interpretation, usually a 2D analysis being considered. The bend over a sheet metal blank consists of a V shape forming by using a punch, with a certain nose radius, forcing the sheet plate against an open die, with a V section. The forming result is a part with an angle obtained between the V legs (flanges), which is known as the bending angle. The operation to get the required V angle is called air bending or free bending [1]. The punch penetration inside the die, known as bending depth, is responsible for the bending angle. However the amount of penetration to reach the required bending angle depends both on the inside bending radius, with direct influence on the geometry for the angle evaluation, and on the amount of springback occurring after releasing the tools from the bent plate.*
In this paper, results are presented describing the use of finite element analysis as an aid in the prediction of the inside bending radius and the expected springback, both influencing punch penetration for the final bending angle. A press brake bending Vt diagram is presented in which forming windows are defined and related to different behaviours and results of bent components. In this diagram a defined forming window is suggested when using a defined material and thickness. Some test results with bent samples are added to evaluate the applicability of the defined approach.

1 INTRODUCTION

The linear bending is one of the most common industrial forming operations. One may find them in electric appliances, such as washing machines, freezers and ovens, in computer frames, in wind mills, lighting towers, ships, trucks and airplanes, etc. A main advantage when using bends in components is the additional stiffness and rigidity to the parts. The bending operations are more commonly made in special long presses called press brakes.

Nowadays most of these machines are fitted with CNC control, an essential capability to suit

the press brake to the actual lean manufacturing management, where the process suitability to small batches and to reliable and repetitive parts is demanded. Also, to avoid frequent tool changes the air bending concept (see section 2) shall be used. As a consequence, the most complete knowledge and understanding on this bending process is paramount to perform the required part at a single stroke (at first trial).

2 BENDING PROCESSES: AIR BENDING

Air bending is the most common bending process and consists of making a linear fold, usually long when compared to the thickness, on a flat blank, by forcing it with a punch nose against an open die that holds the plate as shown in figure 1. In this figure we can see that the linear fold is shown as a *V* shape of variable angle, α.

By assuming this 2D model shown in figure 2 it is possible, through a geometric triangulation, to define the required punch penetration, *y*, to get the bending angle, α. Eq. 1 shows an usual relationship between variables and parameters [1, 2, 3, 4]:

$$y = \frac{V}{2 \cdot \tan(\frac{\alpha}{2})} - (r_i + t) \cdot \frac{1 - \sin(\frac{\alpha}{2})}{\sin(\frac{\alpha}{2})} \tag{1}$$

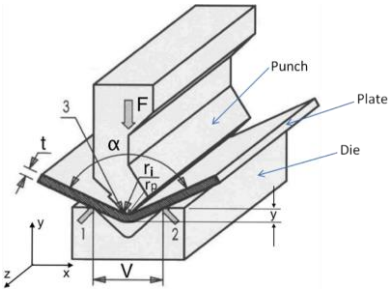

Figure 1 – Main variables in press brake bending.

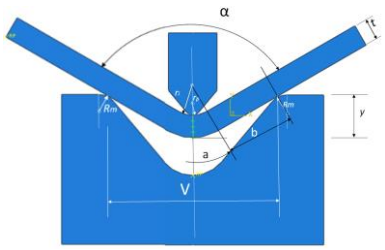

Figure 2 – 2D representation of press brake bending and zones according to a simple rigid plastic model..

However some authors such as De Vin [5, 6, 7, 8] using his rigid plastic model, consider that the punch nose radius r_p is imposing the inside sheet bending radius r_i at the central area, naming this as a "wrap-around" model, being the penetration *y*, a function of the bending angle α and defined as:

$$y = \frac{V}{2 \cdot \tan(\frac{\alpha}{2})} - (r_p + t) \cdot \frac{1 - \sin(\frac{\alpha}{2})}{\sin(\frac{\alpha}{2})} \tag{2}$$[1]

Another approach is proposed by J. Bessa Pacheco [2], in which the corner die radius r_m is taken into account, figure 2, and Eq. (1) turns into Eq. (3) :

$$y = \frac{V}{2 \cdot \tan(\frac{\alpha}{2})} - (r_i + t + r_m) \cdot \frac{1 - \sin(\frac{\alpha}{2})}{\sin(\frac{\alpha}{2})} \tag{3}$$

[1] The original equation was trigonometrically converted by the authors in order to have direct comparisons with equations (1) and (3) written by the authors.

Additionally, there are few expert rules of thumb for air bending [1], with no full freedom to choose any die opening. A main relation includes the die opening, *V*, and the thickness, *t*, which are related by:

$$V = k_{vt} \cdot t \tag{4}$$

with k_{vt} varying between six and ten. On the other hand the inside radius ri is suggested to be given by the die opening, V, divided by 6.4, that is:

$$r_i = \frac{V}{6.4} \tag{5}$$

without making any reference to the sheet metal material in use, but by assuming it is a mild steel.

Even Oehler [9] cites these rules extracted from a Cincinnati (Ohio) press brake catalogue (1949), for mild steel, where it is clear that the inside radius is constant and given by Eq.(4) regardless of the gauge of the metal being formed.

Based on this practice, the ideal rigid plastic model has a geometry expressed by Eq.(1) or (3) that represents rather well the experimental results. Thus, it is the most common and simple model for the air bending representation which, as shown in figure 1 and figure 2, has a central part around the punch nose, where the bending momentum and corresponding bending stress are maximum. This model considers a rigid plastic deformation assuming a cylindrical shape with a constant radius (natural bending radius r_i) and two straight arms or legs departing from the central cylinder and going through the supporting shoulders on the lower die.

By including Eq.(3), (4) and (5) in the CNC of the machine, it is possible to calculate the required penetration to get the target angle α since all the other variables *t*, r_i and r_m are known.

However, this calculation does not include neither the springback effect, nor the change of bending conditions due to tooling dimensions, bending angle or material characteristics. These variables will affect the calculated bending penetration *y*, as well as the targeted bending angle α, thus being necessary the use of trial and error to overcome the faulty parts.

To overcome these successive trial and error operations, many press brake manufacturers have focused through the years in different ways of measuring directly, or indirectly the bending angle during the last steps of the bending process, trying also to take into account the springback. However, the incorporation of these online measuring systems also turns the operation very slow.

Thus, it is of much importance finding a quicker and cheaper way of foreseeing the required punch penetration for the target bending angle α, through a better knowledge of the material behavior during air bending.

As the geometry of the tools is well known, specially the die corner radius r_m, we suppose that the main reason for the angle deviations found on the first bends is not due to the simplicity of the adopted bending model, but on the assumed practical values for the inside bending radius r_i that are faulty and mostly not a fixed value for all the bending angles α.

The bending process comes from the flexure theory. Then the bending moment lowers from a maximum at the center to zero at the die support neighbours. Thus the curvature diminishes correspondingly and consequently the bending radius (the inverse of the curvature) is growing from a minimum at the center to a maximum corresponding to a straight line close to the die shoulders.

Oehler [9] and Lang [11] present in figure 3 the development of the average inside radius r_{im} for the commercial-purity aluminum Al 99,5 w (DIN 1712-3 wrought aluminum alloy grade) bent at a bending angle $\alpha = 90^{o}$:

Also some authors such as De Vin [6, 7] have studied the process introducing the concept of "Three-section models", one wrap around the punch with a r_p radius, another one with a variable radius and a straight one, all coming from the Elasto-Plastic Theory, being the local curvature value based on the local bending moment as illustrated in figure 4.

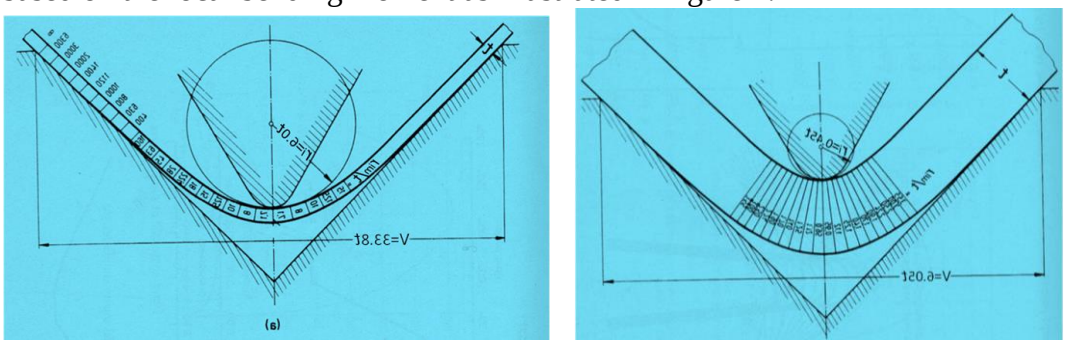

Figure 3 – Development of the average inside radius r_{im} for the commercial-purity aluminum Al 99,5 w bent at a bending angle $\alpha = 90^{o}$ during the air bending for two die openings (V) (Adapted after Oehler [7] and Lang [9].

In this figure 4, we see three types of deformed sections in a bent sheet under loading conditions: (a) a circular section, wrap-around zone under the punch, which has an inner radius equal to the punch radius; (b) an elasto-plastically deformed zone in which the local bend radius varies and that goes further the straight line tangent to the central radius and (c) a zone only elastically deformed that comes to a straight line after springback.

This previous model doesn't seem to correspond to what is observed in experimental bent parts and seen in simulation results. Accordingly, figure 2 and figure 13 show the deformed parts in which we find a circular section (zone a, figure 2) plastic deformed, with an inside radius r_i, followed by a straight line (zone b) tangent to the central arc (a). This last model has a better correspondence with analytical development used for Eq. (3).

This paper deals with the role of the Finite Element Analysis on the confirmation of the validity of the simple model, on the evaluation of inside bending radius r_i that should be used in the model for different bending angles, materials and tools, and finally with the expected springback. This analysis will give the possibility of having better analytic and efficient expressions, which will be of practical interest for the CNC control.

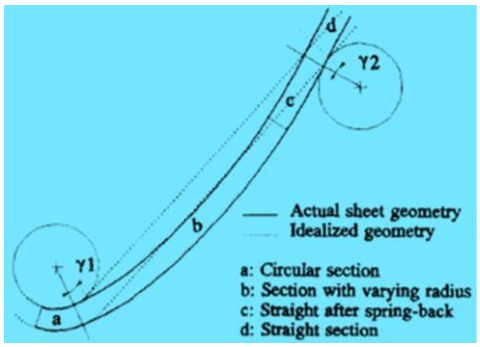

Figure 4 - Sheet geometry according to a 'three section' model.[6, 7]

3 NUMERICAL SIMULATION, TESTS AND MATERIALS

3.1 FEM Analysis

Figure 5 illustrates the basic FEM model used for the different test combinations summarized in Table 1, showing the relative positions between material and tools. Due to symmetry, only half of the real setup is considered. The test combinations, plate dimensions and the geometric parameters on the tools, upper punch and lower die, are also summarized in Table 1. The material characteristics used are described in section and are compiled in Table 2 [2, 3].

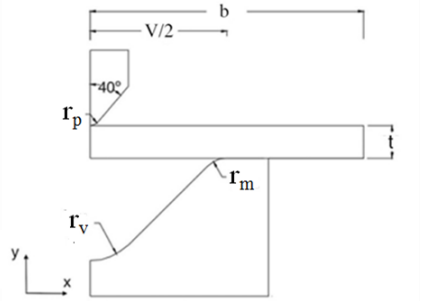

Figure 5 - Numerical model used in FEM.

A 2D FEM model was used with sheet, punch and die discretizations performed by deformable four node solid elements (CPE4R type from ABAQUS® Library).

The bending process was modeled through the dynamic analysis (ABAQUS/Explicit). The sheet plate 2, 3, 4 and 6 mm thick was modeled with 9 layers of 450 solid elements, the punch was modeled with 272 solid elements and the die was modeled 153 solid elements.

Table 1 - FEM test combinations and dimensions for the tooling and flange length.

V opening[2] [mm]	r_p [mm]	*b* [mm]	r_m [mm]	r_v [mm]	Thickness *t* [mm]				
					1	2	3	4	6
11.5	1	15	2	1	x	x	x		
18.3	1	25	2	1	x	x	x	x	
23.1	1	35	2	1	x	x	x	x	x
34.2	1	50	2	1	x	x	x	x	x
53.7	1	50	2	1	x	x	x	x	x

3.2 Press brake Bending Vt Diagram

When performing press brake bending operations there are some relations among variables as expressed, e.g., by Eq. (4) and (5), that should be used or otherwise the bending will not be processed correctly. To illustrate and understand the results when having different relations it is useful using a diagram relating die opening (*V*) vs. blank thickness (*t*) called herein as a Bending *Vt* diagram, figure 6. In this figure each point represents a processing bending with a defined *V* for a defined thickness. Every combination presented in Table 1, is shown in this diagram, figure 6.

[2] The V opening, as initial plate support distance, is presented with decimals that corresponds to the round figures (10, 16, 20, 30, 50) usual in bending tooling charaterization, that corresponds to the shape of a machined sharp V prior to grind the die corner radius

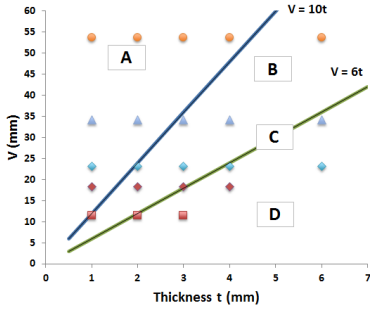

Figure 6 – Press Brake bending *Vt* diagram defining different zones for different *V* vs *t* relations.

In this press brake bending *Vt* diagram we may find four distinct zones, each of them having different characteristics for the bending process but not all of them shall be used when performing press brake bending operations. Figure 7 presents the bent parts obtained for each of these four zones. Zones B and C, for *V/t* between 6 and 10, are those recommended in these kind of operations. Zone A, *V/t* >10, processes bent parts with larger areas of curvature (figure 7) not always fitted to functionality of components, also giving higher elastic recovery (springback). Zone D should be avoided, since parts are prone to local plastic deformation at punch/die contact areas (figure 7), as well as giving severe bending and consequently existing the possibility of damage and fracture for components.

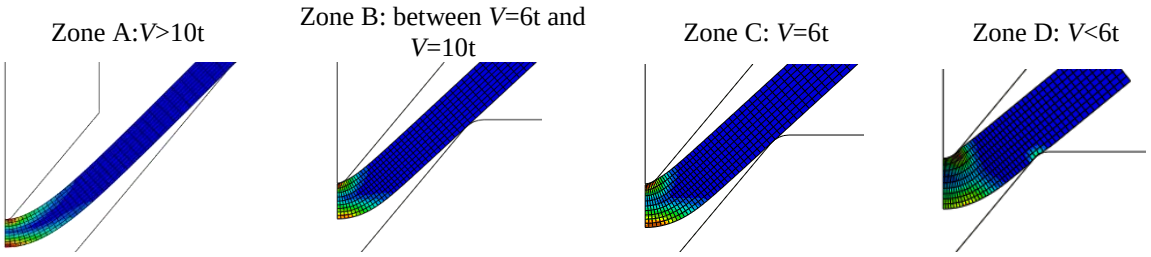

Figure 7 – Bending *Vt* diagram zones

3.3 Materials

Three different materials have been used, two steels (S275JR, DP590) and an aluminum (5182-O), their properties defined in Table 2. The steels were characterized according to Swift law and the 5182 aluminum was characterized by Voce law, the corresponding parameters also presented in Table 2.

Table 2 - Mechanical properties of the tested materials.

	Steel S275JR	**Steel DP590**	**Aluminum 5182-O**
Elastic Modulus - E [GPa]	210	210	69
Poisson coefficient - ν	0.3	0.3	0.3
Proof stress - R_{p02} [MPa]	275	393	143
Tensile Strength - R_m [MPa]	380	641	300
Elongation – [%]	48	26	24
Hardening curve - σ_Y[MPa]	Swift $\sigma=k(\varepsilon_0+\varepsilon)^n$	Swift $\sigma=k(\varepsilon_0+\varepsilon)^n$	Voce $\sigma=\sigma_0+R_{sat}(1-\exp(-Cr*\varepsilon))$
	k = 790 ε_0 =0.013 n=0.245	k = 1000 ε_0 =0.0024 n=0.155	σ_0 = 145.1 R_{sat} = 277.9 Cr = 7.7

4 RESULTS

4.1 Comparison of different analytic approaches

In this section the three different analytical equations expressed by Eq (1), (2) and (3) were used to reproduce the evolution of bending angle with punch displacement and compare with the results obtained from the numerical simulation.

Comparison is made using the materials presented in Table 2, for different blank thicknesses bent on the same *V* die opening (*V=23.1 mm*).

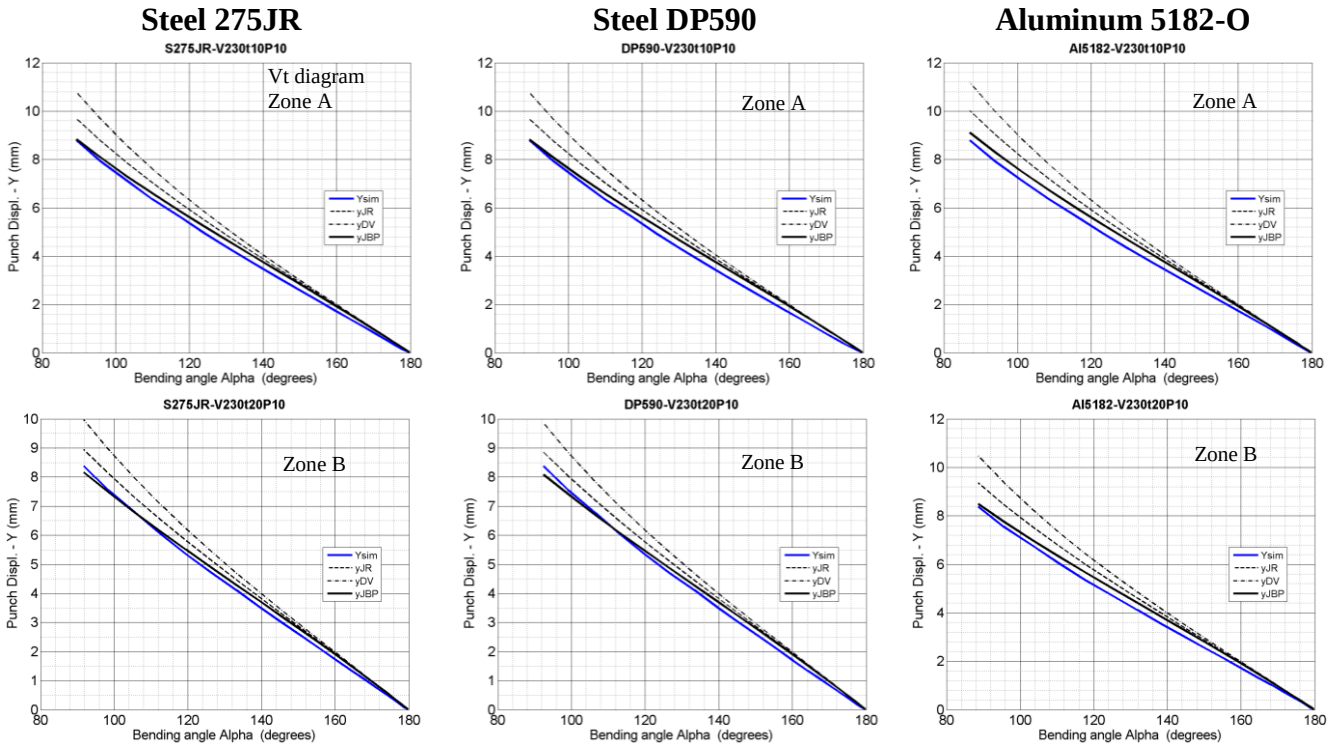

Figure 8 - Comparison of different analytic approaches for the evolution $y=f(\alpha)$ (y_{JR} for Eq. (1), y_{DV} for Eq. (2) and y_{JBP} for Eq. (3)) and the FEM simulation (y_{sim}).

As seen in figure 8, the analytical equation proposed by J. Bessa Pacheco, Eq. (3), has better approach to the evolution obtained from the finite element model for every different zone of *Vt* diagram and different material. This equation includes the die radius (r_m) an important variable to a better accuracy on $y=f(\alpha)$ prediction. For this reason Eq. (3) (*yJBP*) will be the one used for analytical analysis in next sections.

4.2 Evolution of punch displacement (y) versus bending angle (α)

In this section it is considered a more extensive analysis of results obtained by proposed analytical equation (Eq. (3) - *yan*) and it's comparison with simulation results (*ysim*).

An additional analytical equation (*yanc*) is used in which r_i value, instead of being *V/6.4*, Eq. (5), is defined by its calculated value obtained from simulation. In figure 9 the evolution of $y=f(\alpha)$ is presented for *V=23.1 mm* and three materials, while the thickness *t* is increasing from 1 to 4 mm, which means in *Vt* diagram (figure 6) crossing zones A to C.

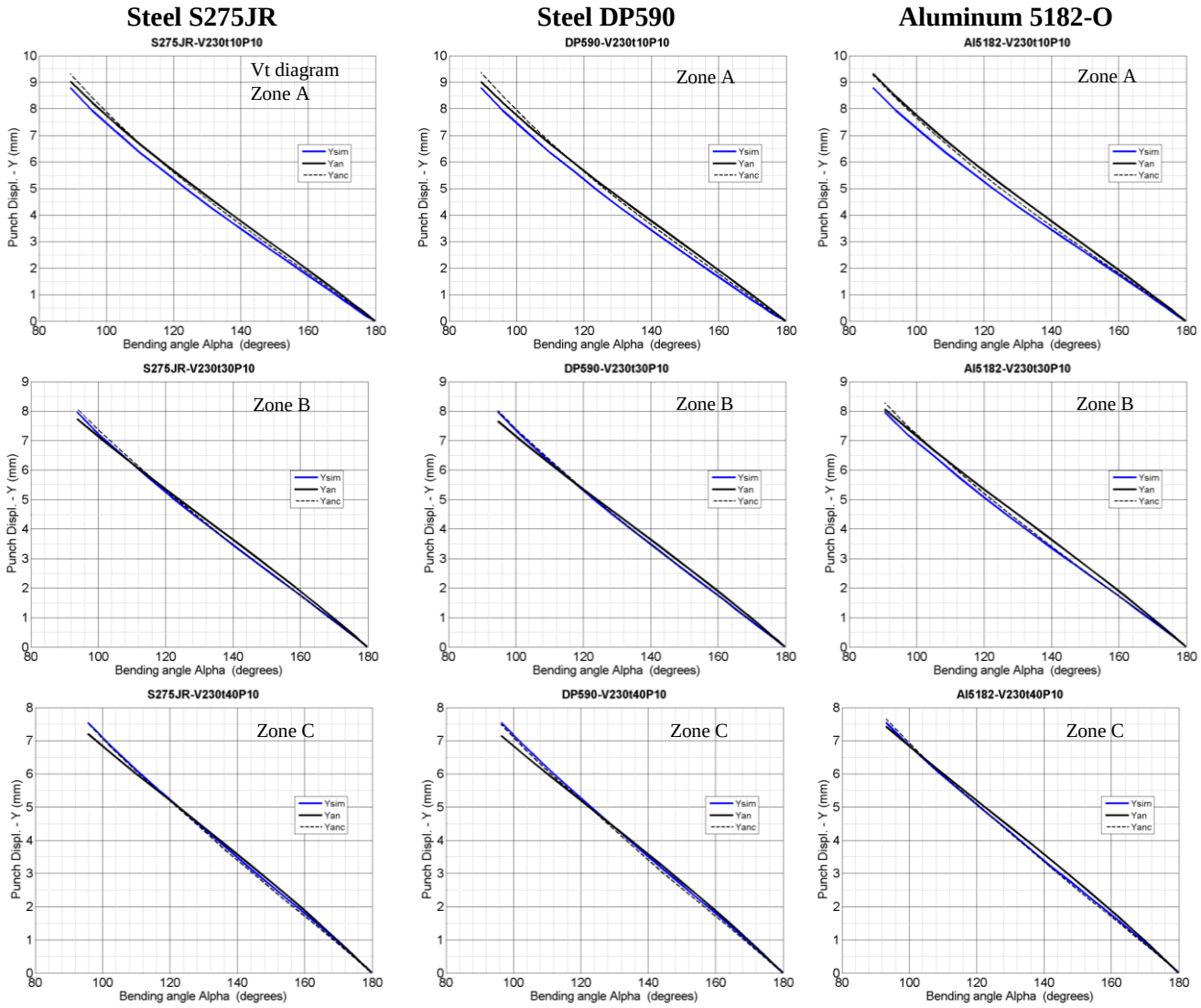

Figure 9 - Evolution of punch displacement (y) versus bending angle (α) for $V=23.1$ *mm* with different materials and different thicknesses (different V/t) corresponding to zones A to C of Vt diagram.

Results for Al5182 in figure 9 show that the behavior of $y=f(\alpha)$ is better predicted by analytic curve when zone C ($V=6t$) is considered. When analyzing these results for other materials (higher strength than Al5182 in consideration) best results are not obtained for zone C ($V=6t$) but a higher V/t value, e.g. $V/t=8$. Therefore, these results suggest different V/t values. Should be used for different materials in order to get the best similarity between analytic curve and simulation results.

4.3 Inside bending radius evolution

A complementary understanding of results for $y=f(\alpha)$ can be performed when analyzing a defined test using other results presented in figure 10. The additional results are ($r_i=f(\alpha)$) inside bending radius vs bending angle, geometrical interpretation of analytic curve vs simulated geometry, as well as stress distribution/deformed geometry of bent component. Such additional

results permit to understand the reasons for the difference between analytic and simulation evolutions.

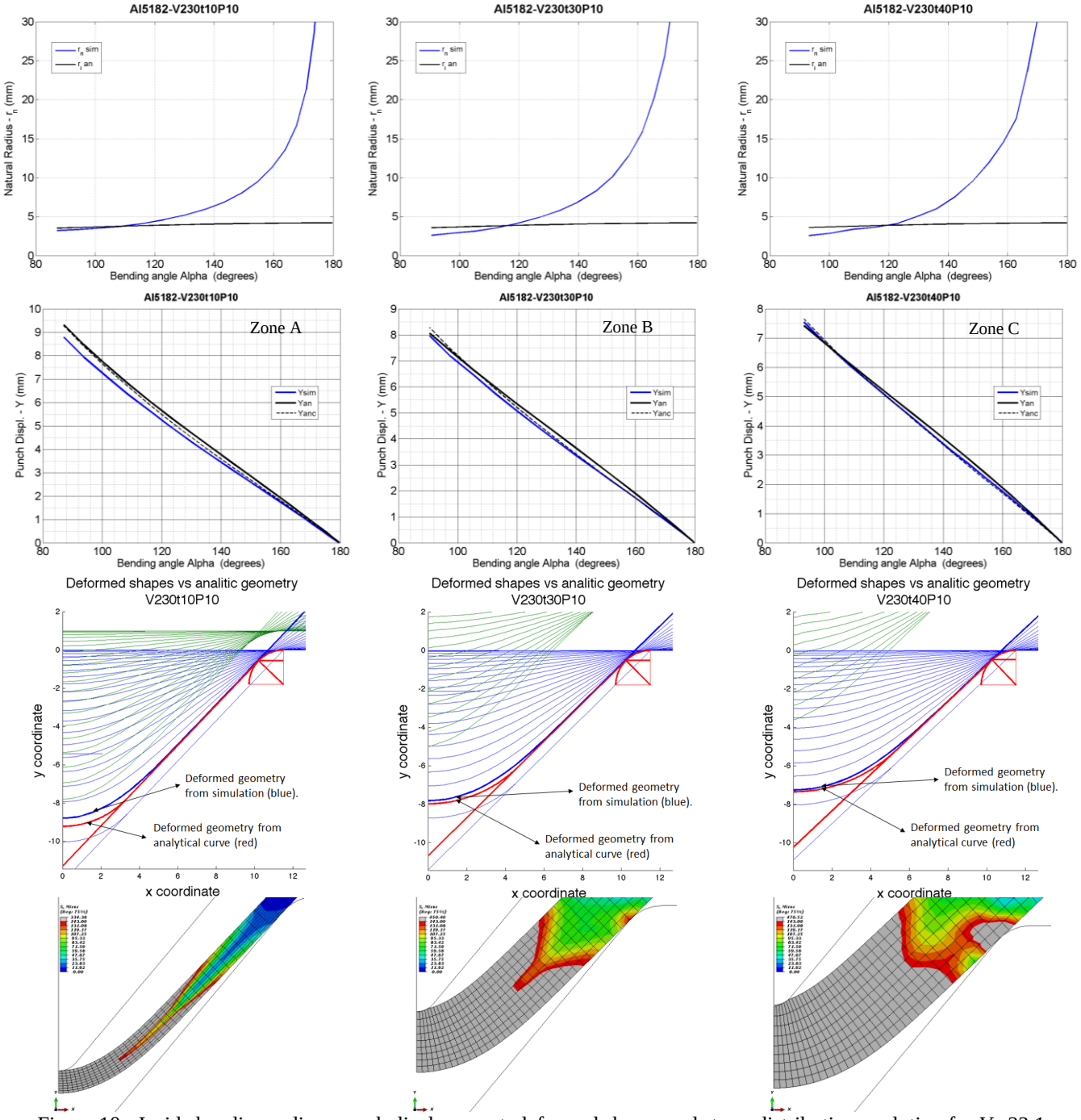

Figure 10 - Inside bending radius, punch displacement, deformed shapes and stress distribution evolution for *V=23.1 mm* and different *V/t* zones, A to C of bending *V/t* diagram.

The results shows that when the *V/t* ratio decrease the simulated geometry (blue) gets closer to the geometrical interpretation of analytic curve (red).

4.4 Punch Force Analysis

For the punch force analysis, a comparison is made between the FEM results and the following expressions, from SSAB (F_{SS})[12] and DIN 6935 (F_{DIN}) [4, 10] respectively:

$$F_{SS} = 1.6 \cdot b \cdot t^2 \cdot \frac{R_m}{V} \quad (6)$$

$$F_{DIN} = (1 + 4\frac{t}{V}) \cdot R_m \cdot \frac{b \times t^2}{V} \quad (7)$$

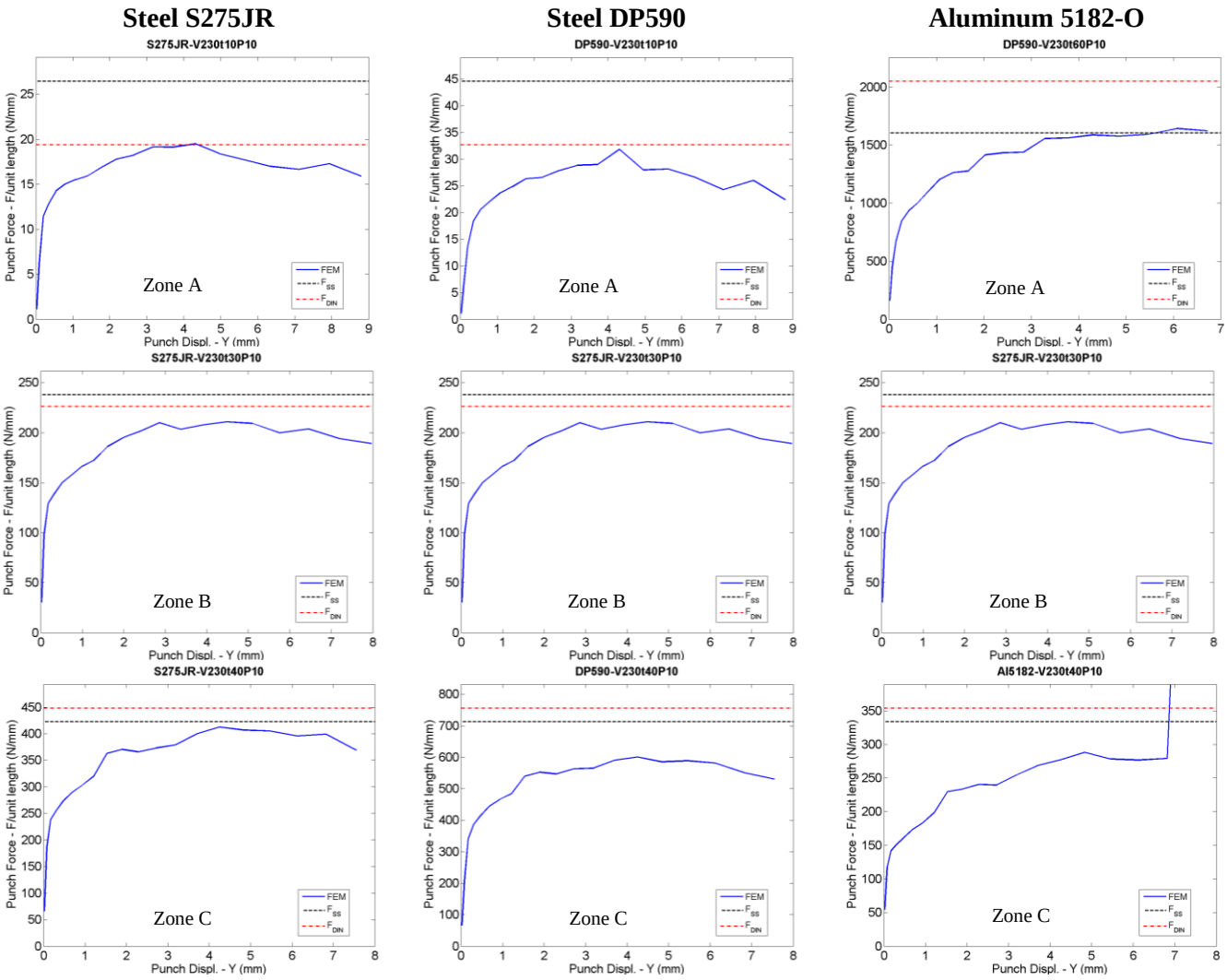

Figure 11 - Evolution of punch force versus punch displacement (y) for V=23.1 mm with different materials and different thicknesses (different V/t) corresponding to zones A to C of Vt diagram.

Relating the punch force with the different zones of the bending *Vt* diagram, the analysis of results (figure 13) shows that for zones B and C the curves obtained by analytic expressions are very close. This is an indication that Eq.(6) is tuned to be used for zones B and C by using a defined *V/t* relation, being these zones the most adequate for press bending operations as already discussed in section 3.2.

4.5 Springback

Springback consists of the bending geometry change after the releasing of the tools from the

bent plate. This happens because the plate, after being bent to a particular curvature coming from a flexing moment created by the loading exerted by the tools, will change its curvature and bending angle after the moment releasing as shown in figure 12.

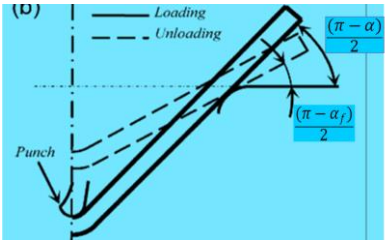

Figure 12 – The springback in the air bending process.

The springback evaluated by (α_f - α) is depending on the material (mechanical characteristics and thickness), tool geometry and the bending angle.

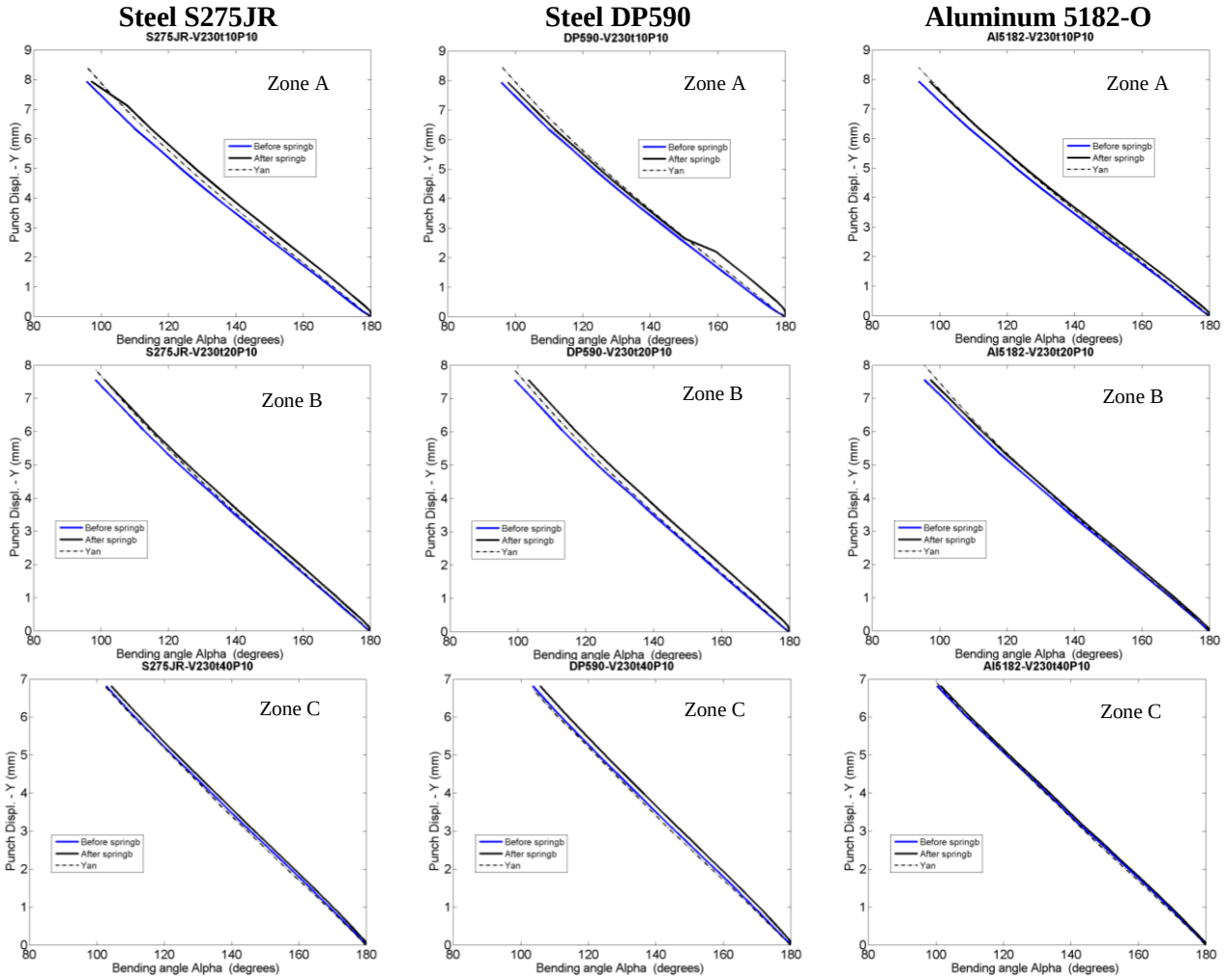

Figure 13 - Evolution of punch displacement (y) versus bending angle (α), in springback, for V=23.1 mm with different materials and different thicknesses (different V/t) corresponding to zones A to C of Vt diagram.

Springback results for Al5182 in figure 13 shows, as expected, that higher elastic recovery is obtained for zone A. When changing bending variables from zone A to C, springback is

continuously decreasing. This is related with stress distribution seen in figure 10. In zone A, the fully plastic region is close to the center line of bending and as V/t relation decreases (from zone A to C), the fully plastic region is increasing, which reduce the stress differential along the thickness, thus reducing the springback.

5 CONCLUSIONS

In this paper it is presented a press bending *Vt* diagram which relates bending zones with heuristics limits *V/t* ratio (6 to 10). An analytic equation is proposed to predict the relation between bending angle and punch penetration while using numerical simulation by FEM as a reference tool to obtain results for press bending process with different tool geometries and materials.

It is shown the influence of each zone of *Vt* diagram on the obtained results, e. g. analytic prediction of bending angle, results for inside bending radius, results of bending force as well as springback.

A diagram relating punch pressure versus *V/t* ratio is also presented which will permit the understanding on the limits of press bending operations thus avoiding local deformations caused by the punch penetration and being able to select a proper punch radius

6 ACKNOWLEDGMENTS

The authors would like to acknowledge the support of FCT - Fundação para a Ciência e a Tecnologia through the projects PTDC/EME-TME/113410/2009 and PTDC/EMS-TEC/2404/2012.

7 REFERENCES

[1] Pacheco J.A.B., Santos A.D., "Numerical Simulation on the validation of a press brake design criteria to minimize angle deviations, CMNE 2011 - Congresso de Métodos Numéricos em Engenharia (2011);

[2] Pacheco J.A.B., Santos A.D., "A study on the Nose Radius influence in Press Brake Bending Operations by Finite Element Analysis", 16th annual ESAFORM 2013, Conference on Material Forming;

[3] Pacheco J.A.B., Santos A.D., "Developments on press brake bending process and limits on analytical expressions based on Numerical Simulation", SEMNI, 2013 - Congreso de Métodos Numéricos en Ingeniería (2013);

[4] Rodrigues J. M. C. e Martins P. A. F., Tecnologia Mecânica ('Mechanical Technology'), Vol. I e Vol.II, Escolar Editora, 2005;

[5] L.J. De Vin, A.H. Streppel, U.P. Singh, H.J.J. Kals, A process model for air bending in CAPP applications, Second International Conference on Sheet Metal, SheMet'94 (1994);

[6] Leo J. De Vin, Computer Aided process Planning for the Bending of Sheet Metal Components, PhD Thesis 1994, University of Twente (NL), ISBN 90-9007217-9;

[7] L.J. De Vin, A.H. Streppel, U.P. Singh, H.J.J. Kals, A process model for air bending, Journal of Materials Processing Technology 57 (1996) 48-54 (1996);

[8] Leo J. De Vin, Curvature prediction in air bending of metal sheet, Journal of Materials Processing Technology 100 (2000) 257-261;

[9] Gerhard Oehler, Biegen unter pressen (Bending and Presses), Carl Hanser Verlag Munchen (1963);

[10] Deutsche Normen, Cold Bending of Flat Steel Product, DIN 6935, October 1975;

[11] Lange, Kurt, Handbook of Metal forming, Mc Graw Hill Book Company (1985).

[12] SSAB, Hardox Weldox bending/shearing Publication, February 2006.